# Synthesis, Characterization, and Physical Properties of Monodisperse Oligo(*p*-phenyleneethynylene)s

**Chuan-Zhen Zhou, Tianxi Liu, Jing-Mei Xu, and Zhi-Kuan Chen***

*Institute of Materials Research and Engineering (IMRE), 3 Research Link, Singapore 117602, Republic of Singapore*

*Received November 4, 2002; Revised Manuscript Received December 10, 2002*

ABSTRACT: A new stepwise synthesis method for the preparation of precisely defined oligo(*p*-phenyleneethynylene)s (OPEs) is described. High-purity monomer, trimer, pentamer, heptamer, and nonamer of OPEs with dihexyloxy side groups and trimethylsilyl (TMS) or thioacetyl (SAc) terminals have been synthesized. The structures of the oligomers were characterized by $^1$H NMR, $^{13}$C NMR, and elemental analysis. DSC studies show narrow and well-developed melting and crystallization peaks, indicating the high perfection of the crystals formed in these oligomers. Optical microscopy was used for investigating the supramolecular morphology of solid-state films of pentamer with TMS end groups, as an example. Numerous dendrites with a spherulitic size of ca. 50 $\mu$m were observed. UV−vis absorption and photoluminescence (PL) spectra in both dilute solution and films show a gradual red shift of the $\lambda_{max}$ from trimer to nonamer. At the nonamer stage, the optical maximum is approaching a limit of convergence.

## Introduction

During the past decade, extensive efforts have been paid to conjugated polymers and their oligomers due to their widely potential applications in electronics, optics, and optoelectronics.[1−3] Recently, research on monodisperse conjugated oligomers has dramatically grown and expanded.[4,5] Monodisperse conjugated oligomers, on one hand, are served as model systems to directly generate useful and predictive structure−property relationships to rationalize the properties of the parent polydisperse polymeric materials.[5,6] On the other hand, oligomer materials with defined length and constitution have become a subject of its own.[7,8] One of the most challenging areas for monodisperse conjugated oligomers is molecular scale electronics, in which single or small packets of molecules will function as the active channels for information transportation, processing, and storage.[9−11] The driving force behind this research is clearly the need for suitable alternative technology to Si-based semiconductors, which is expected to reach its roadblocks in 10−20 years. Utilizing organic molecules to construct electronic devices can surmount the fundamental physical constraints in Si industry and can also result in a rapid and low-cost bottom-up manufacturing process for electronic device fabrication.

Among many molecule-based devices, molecular wire is one of the basic components, which is normally a rigid-rod-like molecular chain with extended electronic conjugation to convey either charge or excited energy from one active unit to another. There have been significant advances in the fabrication and demonstration of molecular electronic wires.[12−16] Oligo(*p*-phenyleneethynylene)s (OPEs), a type of monodisperse and shape-persistent oligomer, is one of the main classes of molecules that have been proposed and demonstrated for use as the wires and other potential backbones of molecular electronic devices.[10] There are three main methods to the syntheses of monodisperse oligo(*p*-phenyleneethynylene)s. One is the solid-phase synthesis approach.[17] The reaction procedures involved are quite simplified because of the omission of time-consuming chromatographic separations of the intermediates as compared to the solution-phase methods. However, purification of the final product is not easy because the incomplete coupling residues on the resins at each step make the final compounds more complicated. Additionally, solid-phase synthesis is limited to preparation in small scale. The second method is the solution-phase iterative divergent/convergent approach. This approach allows doubling the number of repeating units in every three steps, independent of the length of the molecules.[18−20] Nevertheless, because of the mechanism limitation of Pd-catalyzed coupling, the oligomers synthesized through this strategy always contain some diyne byproducts which have the same chain length as the target compounds.[21] The third method is a stepwise approach. This features continuous addition of monofunctional compounds to both ends of a growing chain based on the difference of reactivity of iodine and bromine to alkyne.[22,23] This approach has been proven to be a simple and fast route to short length OPEs using in situ deprotection and coupling reactions. Some insoluble byproducts, however, were obtained because of the undesired but unavoidable oligomerization through alkyne coupling with both iodide and bromide, and the precipitation of the insoluble materials increased with the increase of oligomer chain length.[22]

On the basis of the above knowledge, we designed a new alternative stepwise approach to achieve high-purity OPEs. This method involves only two sets of reaction conditions: desilylation and Pd/Cu-catalyzed coupling. In this paper, we report the synthesis and characterization of a series of hexyloxy-functionalized oligo(*p*-phenyleneethynylene)s with two kinds of different terminal groups. In every two steps, 2,5-dihexyloxy-4-[(trimethylsilyl)ethynyl]iodobenzene or 4-thioacetyliodobenzene was coupled with the diethynyl compounds which were desilylated from the di(trimethylsilyl)ethynyl compounds. Using this approach, undesired oligomerization is avoided and trimer, pentamer, heptamer, and nonamer with trimethylsilyl or thioacetoxy

* Corresponding author: e-mail zk-chen@imre.a-star.edu.sg; phone +65-6874 4331; fax +65-6872 0785.

10.1021/ma021656a CCC: $25.00 
Published on Web 01/30/2003

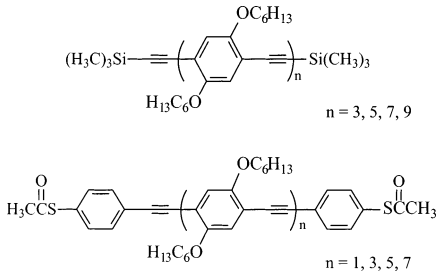


**Figure 1.** Chemical structure of the OPEs.

terminal groups have been obtained readily. Incorporation of thioester groups to the oligomers makes them able to connect with gold surface or electrodes through self-assembly. The chemical structures of the synthesized oligomers are shown in Figure 1. These compounds were fully characterized by $^1$H NMR, $^{13}$C NMR, and elemental analysis. The effect of the chain length on the physical properties was investigated by thermal, absorption, and emission analysis. In addition, the supramolecular morphology of solid-state films of a representative oligomer was studied using optical microscopy.

## Experimental Section

**Materials.** All reagents and solvents were purchased from Aldrich Chemical Co. and Merck. Tetrahydrofuran (THF) was dried over sodium benzophenone. Diisopropylamine was dried over KOH. Both solvents were then distilled under an argon atmosphere and deoxygenated by purging with argon for 30 min before use in oligomer synthesis. All other chemicals were used as received without further purification.

**Methods.** Melting points were determined on a Büchi B-540 capillary melting point apparatus. $^1$H NMR and $^{13}$C NMR spectral data were obtained on a 400 MHz Bruker DPX FT-NMR spectrometer with chloroform-*d* ($CDCl_3$) as solvent and tetramethylsilane (TMS) as the internal standard. EIMS spectra were obtained using a micromass 7034E mass spectrometer. Elemental analyses of all the synthesized compounds were conducted on a Perkin-Elmer 2400 elemental analyzer for C, H, and S determination. The absorption and emission spectra were obtained using a Shimadzu UV-3101 PC UV−vis−NIR spectrophotometer and a Perkin-Elmer LS-50B luminescence spectrophotometer with a xenon lamp as light source, respectively.

The thermal behavior of the oligomers was studied using a differential scanning calorimeter (DSC)-2920 from TA Instruments coupled with a TA-2000 control system. The temperature was accurately calibrated with tin, gallium, and indium using standard procedure. The weights of all the samples were in the range 4−6 mg. All the powdery samples were heated and cooled with a scanning rate of 10 °C/min under a nitrogen atmosphere in order to diminish oxidation.

The powdery sample of oligomer **5b** was dissolved in xylene (at ambient) with a concentration of ca. 1 wt %. The oligomer films were prepared by casting a few drops of xylene solution on glass slides. After evaporation of the solvent, the solid films were used for optical microscopy observation.

**1,4-Dihexyloxybenzene.** A suspension of powdered KOH (50.0 g, 0.9 mol) and anhydrous ethanol (400 mL) was stirred and degassed at room temperature for 30 min. Hydroquinone (38.5 g, 0.35 mol) in anhydrous ethanol (150 mL) was added dropwise. To the stirred mixture, bromohexane (148.0 g, 0.9 mol) in anhydrous ethanol (50 mL) was added. After stirring for 24 h with heating at reflux, the ethanol was evaporated at reduced pressure. The brownish residue was poured into water (500 mL) and extracted with ethyl acetate twice. The combined ethyl acetate layer was washed with water, brine, and dried over anhydrous magnesium sulfate. The white product (74.0 g, 76%) was obtained by recrystallization from ethanol after ethyl acetate was removed under reduced pressure; mp 45.2−46.3 °C. MS *m*/*z*: 278. $^1$H NMR (400 MHz, $CDCl_3$): $\delta$ 6.82 (s, 4H), 3.90 (t, $J$ = 6.6 Hz, 4H), 1.80−1.70 (m, 4H), 1.46−1.30 (m, 12H), 0.90 (t, $J$ = 6.6 Hz, 6H).

**1,4-Dihexyloxy-2,5-diiodobenzene.**[24] To a solution of 1,4-dihexyloxybenzene (11.1 g, 0.04 mol), 90 mL of acetic acid, 7 mL of water, and 3 mL of concentrated $H_2SO_4$ were added $KIO_3$ (10.3 g, 0.048 mol) and $I_2$ (13.1 g, 0.048 mol). The reaction mixture was stirred at 80 °C for 24 h and then cooled to room temperature. After most of the acetic acid was evaporated under reduced pressure, aqueous $Na_2SO_3$ (20%) was added until the brown color of iodine had disappeared. The mixture was poured into ice water with $Na_2CO_3$ (500 mL) and extracted with hexane (3 × 200 mL). The combined organic layer was washed with water and brine and dried over $MgSO_4$. The solvent was evaporated under reduced pressure to give a yellow solid. The white crystals (12.7 g, 60%) were obtained by recrystallization from ethanol; mp 59.9−60.7 °C. MS *m*/*z*: 530. $^1$H NMR (400 MHz, $CDCl_3$): $\delta$ 7.17 (s, 2H), 3.92 (t, $J$ = 6.6 Hz, 4H), 1.84−1.75 (m, 4H), 1.55−1.34 (m, 12H), 0.91 (t, $J$ = 6.6 Hz, 6H). $^{13}$C NMR (100 MHz, $CDCl_3$): $\delta$ 152.85, 122.80, 86.29, 70.34, 31.43, 29.09, 25.68, 22.55, 13.99.

**2,5-Dihexyloxy-4-[(trimethylsilyl)ethynyl]iodobenzene (1a).**[25] To a solution of 1,4-dihexyloxy-2,5-diiodobenzene (7.95 g, 0.015 mol), CuI (0.14 g, 0.75 mmol), and $Pd(PPh_3)_2Cl_2$ (0.53 g, 0.75 mmol) in 100 mL of diisopropylamine was added (trimethylsilyl)acetylene (1.47 g, 0.015 mol). The mixture was stirred at room temperature for 15 h. After removal of the solvent under reduced pressure, a light yellow oil (**1a**; 3.30 g, 44%) was separated from starting material and byproduct by column chromatography using silica gel with hexane/$CH_2Cl_2$ (20:1) as eluent. MS *m*/*z*: 500. $^1$H NMR (400 MHz, $CDCl_3$): $\delta$ 7.04 (s, 1H), 6.94 (s, 1H), 3.96−3.91 (m, 4H), 1.84−1.72 (m, 4H), 1.56−1.33 (m, 12H), 0.91 (t, $J$ = 6.6 Hz, 6H), 0.25 (s, 9H).

**1,4-Bis[(trimethylsilyl)ethynyl]-2,5-bis(hexyloxy)benzene (1b).**[24] To a solution of 1,4-dihexyloxy-2,5-diiodobenzene (7.95 g, 0.015 mol), CuI (0.14 g, 0.75 mmol), and $Pd(PPh_3)_2Cl_2$ (0.53 g, 0.75 mmol) in 100 mL of diisopropylamine was added (trimethylsilyl)acetylene (2.94 g, 0.03 mol). The mixture was stirred at reflux for 1 h. After cooling, dichloromethane (100 mL) was added, and the white ammonium iodide precipitate was filtered off. The solution was passed through a short silica gel column using toluene as eluent. After the solvent was evaporated under reduced pressure, the white crystals **1b** (6.3 g, 89%) were obtained by recrystallization from ethanol; mp 91.0−91.5 °C. MS *m*/*z*: 470. $^1$H NMR (400 MHz, $CDCl_3$): $\delta$ 6.88 (s, 2H), 3.93 (t, $J$ = 6.6 Hz, 4H), 1.81−1.76 (m, 4H), 1.53−1.33 (m, 12H), 0.88 (t, $J$ = 6.6 Hz, 6H), 0.25 (s, 18H). $^{13}$C NMR (100 MHz, $CDCl_3$): $\delta$ 154.45, 117.75, 114.45, 101.50, 100.43, 69.92, 31.99, 29.70, 26.07, 23.01, 14.43, 0.33.

**General Procedure for the Preparation of 1c, 3c, 5c, and 7c.**[24] Methanol and NaOH (5 N) were added at room temperature to a stirred THF solution of **1b**, **3b**, **5b**, and **7b**. The reaction mixture was stirred for 2 h. After removal of the solvent under reduced pressure, **1c**, **3c**, **5c**, and **7c** were separated by column chromatography, respectively.

**1,4-Bis(ethynyl)-2,5-bis(hexyloxy)benzene (1c).** The above general procedure was applied on methanol (30 mL) and NaOH (2 mL, 5 N) in a stirred solution of **1b** (2.82 g, 0.006 mol) in THF (20 mL). The solvent was evaporated, and the residue was poured into 100 mL of water and extracted with hexane twice. The combined hexane layer was washed with water and brine and dried over anhydrous magnesium sulfate. The pale yellow solid **1c** (1.82 g, 93%) was obtained after the solvent was removed; mp 71.1−72.0 °C. MS *m*/*z*: 326. $^1$H NMR (400 MHz, $CDCl_3$): $\delta$ 6.95 (s, 2H), 3.97 (t, $J$ = 6.6 Hz, 4H), 3.33 (s, 2H), 1.84−1.75 (m, 4H), 1.50−1.26 (m, 12H), 0.90 (t, $J$ = 6.6 Hz, 6H). $^{13}$C NMR (100 MHz, $CDCl_3$): $\delta$ 154.43, 118.26, 113.75, 82.75, 80.19, 70.13, 31.90, 29.50, 25.97, 22.96, 14.37.

The data of deprotected trimer (**3c**), pentamer (**5c**), and heptamer (**7c**) could be found in the Supporting Information.

**General Procedure for Preparation of 3b, 5b, 7b, and 9b.** A mixture of diethynyl compound (**1c**, **3c**, **5c**, and **7c**), 2.5 mole ratio of 2,5-dihexyloxy-4-[(trimethylsilyl)ethynyl]iodobenzene, 10 mol % CuI, 10 mol % $Pd(PPh_3)_2Cl_2$, and mixed solvents of diisopropylamine/THF was stirred at room tem-

**Scheme 1. Synthetic Routes to Trimethylsilyl- or Thioester-Terminated OPEs**[a]

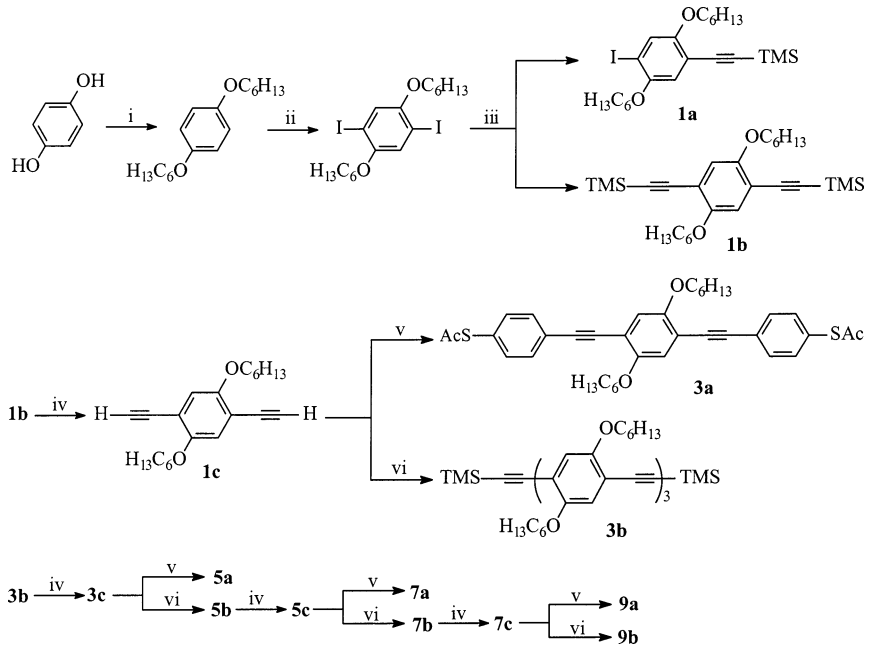


[a] Reagents and conditions: (i) bromohexane, KOH/EtOH, reflux, 24 h; (ii) $KIO_3$, $I_2$, $AcOH/H_2SO_4/H_2O$, 80 °C, 24 h; (iii) $Pd(PPh_3)_2Cl_2$ (10 mol %), CuI (10 mol %), $^iPr_2NH$, trimethylsilylacetylene, reflux, 1 h; (iv) MeOH/THF, 5 N NaOH, rt, 2 h; (v) 1-iodo-4-thioacetylbenzene, $Pd(PPh_3)_2Cl_2$ (10 mol %), CuI (10 mol %), $^iPr_2NH$/THF, rt, 15 h; (vi) **1a**, $Pd(PPh_3)_2Cl_2$ (10 mol %), CuI (10 mol %), $^iPr_2NH$/THF, rt, 15 h.

perature for 15 h. After removal of the solvent under reduced pressure, **3b**, **5b**, **7b**, and **9b** were separated by column chromatography, respectively.

**TMS-Terminated Trimer (3b).** The general procedure mentioned was applied on **1c** (1.63 g, 5 mmol), 2,5-dihexyloxy-4-[(trimethylsilyl)ethynyl]iodobenzene (**1a)** (6.25 g, 12.5 mmol), CuI (0.095 g, 0.5 mmol), and $Pd(PPh_3)_2Cl_2$ (0.351 g, 0.5 mmol) in 60 mL of diisopropylamine and 30 mL of THF. The bright yellow solid **3b** (4.82 g, 90%) was obtained after chromatography using silica gel with hexane/$CH_2Cl_2$ (4:1) as eluent; mp 109.5−110.6 °C. $^1$H NMR (400 MHz, $CDCl_3$): $\delta$ 7.01 (s, 2H), 6.98 (s, 2H), 6.96 (s, 2H), 4.05−3.97 (m, 12H), 1.87−1.84 (m, 12H), 1.59 − 1.53 (m, 12H), 1.36−1.28 (m, 24H), 0.93−0.88 (m, 18H), 0.28 (s, 18H). $^{13}$C NMR (100 MHz, $CDCl_3$): $\delta$ 154.60, 153.92, 153.79, 117.92, 117.73, 117.53, 115.03, 114.74, 114.15, 101.62, 100.47, 91.93, 91.83, 70.12, 69.91, 32.01, 29.70, 26.07, 23.02, 14.41, 0.36. Anal. Calcd for $C_{68}H_{102}O_6Si_2$: C, 76.21; H, 9.59. Found: C, 76.34; H, 9.75.

The data of TMS-terminated pentamer (**5b**), heptamer (**7b**), and nonamer (**9b**) could be found in the Supporting Information.

**General Procedure for the Preparation of 3a, 5a, 7a, and 9a.** A mixture of diethynyl compounds (**1c**, **3c**, **5c**, and **7c**), 2.5 mole ratio of 1-iodo-4-thioacetylbenzene, 10 mol % CuI, 10 mol % $Pd(PPh_3)_2Cl_2$, and mixed solvents of diisopropylamine/THF was stirred at room temperature for 15 h. After removal of the solvent under reduced pressure, **3a**, **5a**, **7a**, and **9a** were separated by column chromatography, respectively.

**Thioester-Terminated Trimer (3a).** The general procedure mentioned was applied on **1c** (0.39 g, 1.19 mmol), 1-iodo-4-thioacetylbenzene (0.69 g, 2.5 mmol), CuI (0.023 g, 0.119 mmol), and $Pd(PPh_3)_2Cl_2$ (0.084 g, 0.119 mmol) in 60 mL of diisopropylamine. The bright yellow solid **3a** (0.50 g, 67%) was obtained after chromatography using silica gel with hexane/$CH_2Cl_2$ (2:1) as eluent; mp 112.5−113.7 °C. $^1$H NMR (400 MHz, $CDCl_3$): $\delta$ 7.56 (d, $J$ = 8.0 Hz, 4H), 7.40 (d, $J$ = 8.0 Hz, 4H), 7.01 (s, 2H), 4.04 (t, $J$ = 6.6 Hz, 4H), 2.44 (s, 6H), 1.87−1.83 (m, 4H), 1.58−1.53 (m, 4H), 1.36−1.26 (m, 8H), 0.90 (t, $J$ = 6.6 Hz, 6H). $^{13}$C NMR (100 MHz, $CDCl_3$): $\delta$ 193.78, 154.20, 134.55, 132.50, 128.48, 125.14, 117.45, 114.42, 94.55, 88.09, 70.11, 31.97, 29.71, 26.12, 23.01, 14.40. Anal. Calcd for $C_{38}H_{42}O_4S_2$: C, 72.81; H, 6.75; S, 10.23. Found: C, 73.21; H, 7.26; S, 9.74.

The data of thioester-terminated pentamer (**5a**), heptamer (**7a**), and nonamer (**9a**) could be found in the Supporting Information.

## Results and Discussion

Since many applications require only short but highly pure and easily processable oligomeric systems, we designed a novel stepwise approach, which allows purification of each intermediate and then ensures the high purity of the resulting oligomers. The synthetic procedure for the dihexyloxy-substituted OPEs is depicted in Scheme 1. The procedure involves only two types of reaction conditions: desilylation and Pd/Cu-catalyzed coupling reaction. The initial 2,5-dihexyloxy-1,4-diiodobenzene was obtained by iodination of the 1,4-dihexyloxybenzene. Treatment of 2,5-dihexyloxy-1,4-diiodobenzene with one and two molar amount of (trimethylsilyl)acetylene gave 2,5-dihexyloxy-4-[(trimethylsilyl)ethynyl]-iodobenzene (**1a**) and 2,5-dihexyloxy-1,4-bis[(trimethylsilyl)ethynyl] benzene (**1b**), respectively. Removal of the protection group of **1b** generated the desilylated 2,5-dihexyloxy-1,4-bis(ethynyl)benzene (**1c**). Pd/Cu-catalyzed coupling of **1c** with 1-iodo-4-thioacetylbenzene or **1a** gave trimer **3a** with thioester end groups or trimer **3b** with trimethylsilyl end groups. Since **3b** has the same TMS protected alkyne end groups as **1b**, the desilylation and coupling reactions can be iterated. By repeating the reaction sequence, oligomers up to nine repeating units with thioester (**3a**, **5a**, **7a**, and **9a**) and −TMS (**3b**, **5b**, **7b**, and **9b**) terminals have been obtained readily using the same reaction conditions. A 2.5 molar ratio of compound 1-iodo-4-thioacetylbenzene or **1a** was added to the Pd/Cu-catalyzed coupling reaction to ensure the completion of the starting materials and help to ease the isolation of the products. All the oligomers possess very good solubility in common organic solvents. The thioester terminals attached to the oligomers can serve as alligator clips for adhesion to gold surfaces or gold nanoelectrodes so that the wiring

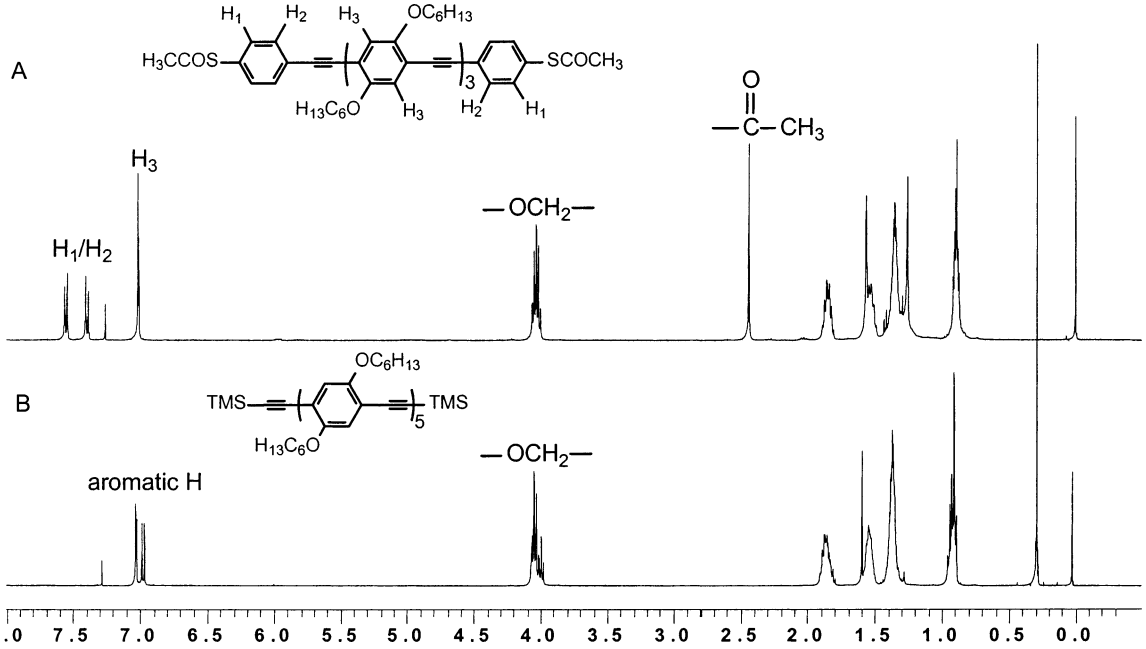


**Figure 2.** Representative $^1$H NMR spectra of **5a** and **5b** in $CDCl_3$.

function can be realized, and their transportation of signals can be measured.

The structure and purity of the obtained OPEs were characterized by $^1$H NMR, $^{13}$C NMR, and elemental analysis. The representative $^1$H NMR spectra of **5a** and **5b** are depicted in Figure 2. It can be seen in Figure 2A ($^1$H NMR of **5a**) that there are two doublets at around 7.55 and 7.40 ppm, which are assigned to the protons on the thioester-substituted benzene rings. The peak at 7.01 ppm is assigned to the protons on the middle hexyloxy-substituted benzene rings. The ratio of the integration of the three distinct aromatic signals at 7.55, 7.44, and 7.01 is 2:2:3, indicating the length and structure of the expected pentamer **5a**. Figure 2B shows the $^1$H NMR spectrum of **5b**. The peaks at around 7.00 ppm are attributed to the protons of the five symmetric aromatic rings. The signal at 0.26 ppm is the characteristic peak of −TMS. The ratio of the intensities of $-Si(CH_3)_3$ and the aromatic protons is 9:5, which agrees with the calculated ratio of the oligomer **5b**.

The DSC heating (A) and cooling (B) curves of oligomers **3b**, **5b**, **7b**, and **9b** are shown in Figure 3. For the purpose of comparison, all the DSC curves are normalized by weight and shifted vertically for clarification. It can be seen that the endothermic melting peaks (in Figure 3A) systematically shift toward higher temperatures (from 116 °C to 147, 168, and 185 °C for **3b**, **5b**, **7b**, and **9b**, respectively) with increasing repeating units of oligomers, whereas the magnitudes of the melting peaks gradually decrease as repeating units increases, indicating a systematic reduction in perfection of the crystals formed. After the heating scan (Figure 3A), the samples were kept at their respective melts (200 or 250 °C) for 5 min under nitrogen to eliminate thermal history and then cooled at the same rate. For the cooling scan (Figure 3B), the exothermic crystallization peaks shift toward higher temperatures (from 94 °C to 122, 143, and 168 °C for **3b**, **5b**, **7b**, and **9b**, respectively). Meanwhile, the same trend of decreasing peak magnitude was observed with increasing repeating units. Compared with PPEs, which have shown liquid crystalline behavior,[26] the narrow and well-developed melting and crystallization peaks indicate the high perfection of the crystals formed and the well-defined structures of these oligomers.

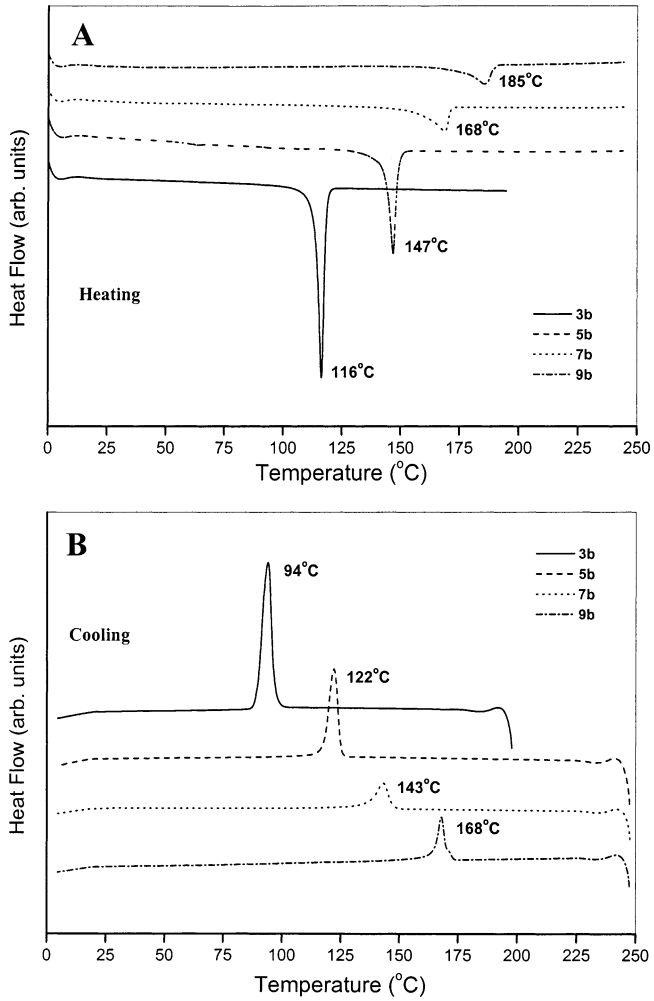


**Figure 3.** DSC heating (A) and cooling (B) curves of TMS-terminated OPEs.

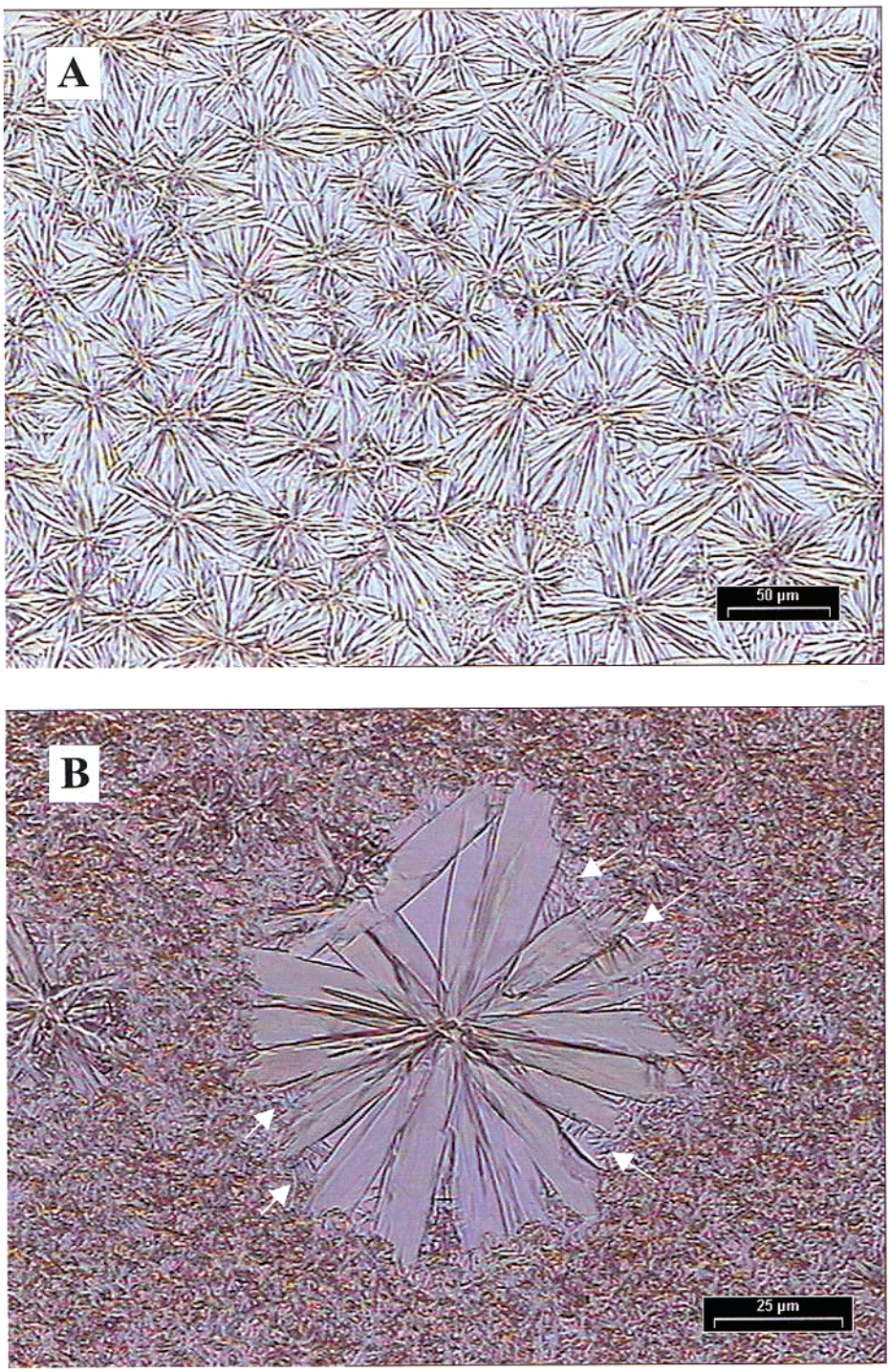


**Figure 4.** Optical micrographs of self-organized supramolecular morphology of **5b** on glass: (A) dendrite crystals and (B) lathlike crystals.

Organic molecular crystals are promising candidates for molecular electronic devices. Before such devices can be realized, however, a better understanding of the structural factors that control the electronic and optical properties of organic solids is needed.[27] The supramolecular morphology of solid-state films of oligomer **5b**, as an example, was studied using optical microscopy. The self-organized crystalline morphology of **5b** on glass is shown in Figure 4. Numerous dendrites with a spherulitic size of ca. 50 $\mu$m are observed (Figure 4A). Nevertheless, because of high nucleation density, the further growth of the dendritic crystals is restricted, and consequently the morphological details are somewhat concealed. In some areas with low nucleation density, large axialites grown from isolated nuclei are occasionally observed, consisting of several to tens of lathlike crystals with smooth surfaces which fan out in typical axialitic fashion to form a full spherulite (Figure 4B). These laths are usually 30−50 $\mu$m long and 5−10 $\mu$m wide. It can also be seen that the lathlike crystal sheets have rather regular (lateral) edges but irregular growth tips probably due to the uneven accumulation of rejected species during crystal growth. Occasionally, some multilayer overgrowths on the laths are observed upon closer inspection. In addition, as indicated by arrows, some minute needlelike crystals always appear oriented

**Table 1. Optical Properties of TMS- and Thioester-Terminated OPEs**

| | $\lambda_{max}$ (UV nm) | | $\lambda_{max}$ (PL nm) | | |
|---|---|---|---|---|---|
| oligomer | solution | film | solution[a] | film[a] | $\Delta\lambda_{max}$ (nm)[b] |
| trimer−SAc (**3a**) | 378 | 391, 411 | 415 (433) | 466 | |
| pentamer−SAc (**5a**) | 410 | 423, 436, 462 | 450 (477) | (480) 504 | 35 |
| heptamer−SAc (**7a**) | 421 | 435, 447, 472 | 463 (492) | (497) 521 | 13 |
| nonamer−SAc (**9a**) | 431 | 440, 453, 480 | 467 (500) | (504) 528 | 4 |
| trimer−TMS (**3b**) | 397 | 401, 413, 435 | 434 (457) | 480 (517) | |
| pentamer−TMS (**5b**) | 413 | 425, 437, 461 | 457 (486) | (494) 508 (532) | 23 |
| heptamer−TMS (**7b**) | 425 | 434, 448, 471 | 466 (494) | 523 (544) | 9 |
| nonamer−TMS (**9b**) | 430 | 438, 452, 476 | 468 (496) | (500) 530 | 2 |

[a] The values in parentheses refer emission shoulders. [b] $\Delta\lambda_{max}$ is the difference of the emission maximum from $n$ to $n + 2$.

transversely to the outer parts of the edges of the underlying laths where the distance between the neighboring laths is widely spaced. That is, the lateral growth of these tiny crystals is normal to the growth direction of the underlying lath crystals, resembling a homoepitaxial growth habit. Similar axialitic and lathlike crystal morphologies were also observed in syndiotactic polypropylene (sPP) using transmission electron microscopy (TEM) by Lovinger et al.[28] and using atomic force microscopy (AFM) by Tsukruk et al.[29] Under lower solution concentration (such as 0.1−0.5 wt %), our preliminary TEM and AFM results have shown that more perfect and larger single crystals can be obtained from dilute xylene solutions with lath length exceeding several hundred micrometers and width of ca. tens of micrometers.[30] Currently, the preparation of single-crystal thin films and the structural determination of single crystals of the synthesized oligomers are still under way.

UV−vis absorption and photoluminescence (PL) spectra of the dilute solution of THF and thin films of OPEs were measured. The wavelengths of the peaks are summarized in Table 1. The demonstrative UV and PL spectra of the oligomers with −TMS terminal groups in solutions and solid states are shown in parts A and B of Figure 5, respectively. As expected, an increase in the absorption and emission maxima from shorter wavelength 397 and 434 nm for the trimer **3b** to the longer wavelength 430 and 468 nm for the nonamer **9b** in dilute THF solution was observed. The bathochromic shift of emission from trimer **3b** to pentamer **5b** is 23 nm, while that of emission from heptamer **7b** to nonamer **9b**, however, is only 2 nm. These results indicate that the $\lambda_{max}$ values of both UV absorption and PL emission are approaching a limit of convergence at the nonamer stage, and this tendency is illustrated in Figure 5A,B. Indeed, the wavelengths of maximal absorption and emission of **9b** in THF are even higher than its polymer counterparts with didecyloxy or didodecyloxy side chains measured at the same conditions.[21,31] This is in agreement with the observation of dipropoxy-substituted OPEs, which showed the saturated absorption and emission at the decamer stage.[32,33] From Figure 5A, it can be found that each of the absorptions of these −TMS-terminated OPEs in dilute THF solution appear as a broad peak with one maximum. The PL spectra in solution exhibit one maximum peak and one shoulder, which is red-shifted about 28 nm to their corresponding maximum. It is also noted that the oligomer emission bands are much narrower than the absorption bands, which is consistent with emission from localized excited states.[34,35]

Figure 5B shows the UV−vis absorption and photoluminescence (PL) spectra of the four −TMS-terminated OPEs in thin films. The films were spin-cast onto quartz

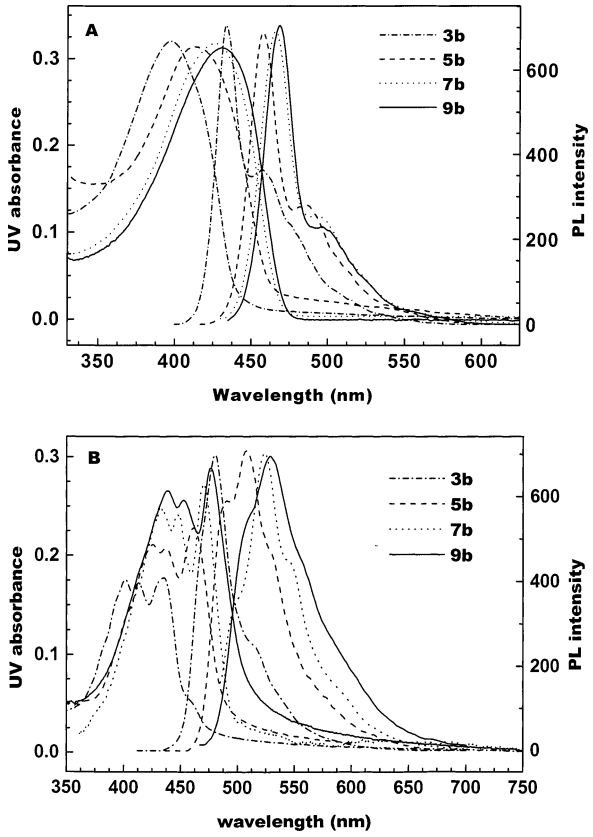


**Figure 5.** UV−vis absorption and photoluminescence spectra of TMS-terminated OPEs in (A) THF solution and (B) solid state.

plates from their solutions in THF (2 wt %). All the films prepared are visibly uniform and emit blue-green to green fluorescence. It is noted that the absorption spectra of the oligomers in solid states exhibit significant changes compared with those in dilute solutions. There are three highly structured absorption peaks in the UV spectra. For example, the three peaks for **5b** center at 425, 437, and 461 nm in wavelength or 2.918, 2.838, and 2.690 eV in energy. The well-resolved structure of the absorption spectra is ascribed to the highly ordered organization of the oligomers in solid state, which has been illustrated in optical micrographs and DSC thermograms. The high ordering in thin films should be attributed to the $\pi-\pi$ stacking of the oligomer backbones and also the hydrophobic interactions between alkoxy side chains. Among the three well-resolved peaks, the right dominant peak is assigned to the lowest singlet ($^1$Bu) exciton transition (0−0), i.e., the transition from the ground state to the relaxed excitation state in conjugated oligomers. Others are its vibronic sidebands.[36−39] The energy space between the 0−0 (right peak) and 0−1 (middle peak) transitions, corresponding

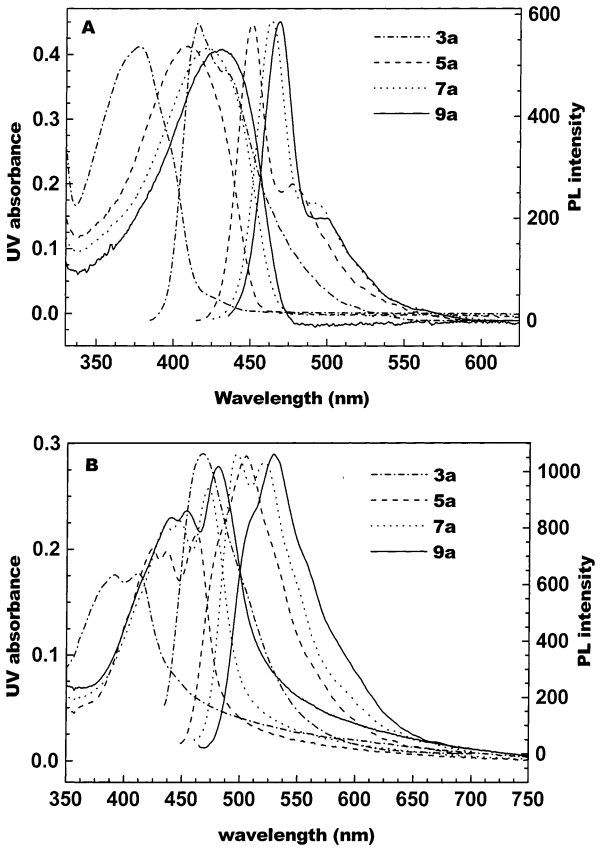


**Figure 6.** UV−vis absorption and photoluminescence spectra of thioester-terminated OPEs in (A) THF solution and (B) solid state.

to C═C stretching vibration, is around 150 meV, which is a typical value and had been reported in other conjugated polymer systems.[40−42] The PL spectra of the −TMS-terminated OPEs in thin films show less structured feature and peak at 480, 508, 523, and 530 nm for the four oligomers. Comparing the maximal emission and absorption in film states to their solutions, it can be noted that the red shift for the both cases is about 40−60 nm. These results indicate strong intermolecular interaction in the solid state.[43]

The oligomers with thioacetyl terminal groups have similar optical properties as those with −TMS terminal groups. The detailed absorption and emission wavelengths of the peaks are summarized in Table 1. The absorption maxima of the −SAc-terminated OPEs in THF solution are 378, 410, 421, and 431 nm. Except for **3a**, there are no obvious differences in the absorption maxima compared with those of −TMS-terminated OPEs, which show maxima at 397, 413, 425, and 430 nm. Similar to the absorption spectra of **3b**−**9b** in solid thin films, those of **3a**−**9a** also show three highly structured peaks. Both of the UV absorption and PL emission spectra have similar trends as −TMS-terminated OPEs: the $\lambda_{max}$ values of both absorption and emission are approaching a limit of convergence at the nonamer stage, which is illustrated in Figure 6A,B.

## Conclusions

Two series of oligo(*p*-phenyleneethynylene)s (OPEs) with either trimethylsilyl end groups or thioacetyl terminals have been prepared through a new stepwise synthetic method. Pure oligomers with chain lengths up to nonamer were easily synthesized. Absorption and photoluminescence spectroscopy investigation of the oligomers indicates that the bathochromic shift of optical maximum is approaching a limit of convergence when the oligomer chain length increases from trimer to nonamer. DSC and optical microscopy studies reveal that oligomers with trimethylsilyl end groups form dendrite crystals with high perfection. Lathlike crystal sheets with length of several hundred micrometers and width of tens of micrometers have been observed, which may be applicable for high mobility field effect transistors through a simple and cheap solution process. The application of oligomers with thioester end groups as molecular wires is still under investigation.

**Supporting Information Available:** Synthesis and analytical data of intermediate compounds of **3c**, **5c**, and **7c**, the TMS-terminated oligomers of **5b**, **7b**, and **9b**, and also the thioester-terminated oligomers of **5a**, **7a**, and **9a**. This material is available free of charge via the Internet at http://pubs.acs.org.

## References and Notes

(1) Skotheim, T. A.; Elsenbaumer, R. L.; Reynolds, J. R. *Handbook of Conducting Polymers*, 2nd ed.; Marcel Dekker: New York, 1998.
(2) Scherf, U. *Top. Curr. Chem.* **1999**, *201*, 163.
(3) Segura, J. L.; Martin, N. *J. Mater. Chem.* **2000**, *10*, 2403.
(4) Müllen, K.; Wegner, G. *Electronic Materials: the Oligomer Approach*; Wiley-VCH: Weinheim, 1997.
(5) Martin, R. E.; Diederich, F. *Angew. Chem., Int. Ed.* **1999**, *38*, 1350.
(6) Van Hutten, P. F.; Krasnikov, V. V.; Hadziioannou, G. *Acc. Chem. Res.* **1999**, *32*, 257.
(7) Katz, H. E.; Bao, Z.; Gilat, S. L. *Acc. Chem. Res.* **2001**, *34*, 359.
(8) Fichou, D. *J. Mater. Chem.* **2000**, *10*, 571.
(9) Tour, J. M.; Reinerth, W. A.; Jones, L.; Burgin, T. P.; Zhou, C. W.; Muller, C. J.; Deshpande, M. R.; Reed, M. A. *Ann. N.Y. Acad. Sci.* **1998**, *852*, 197.
(10) Tour, J. M. *Acc. Chem. Res.* **2000**, *33*, 791.
(11) Reed, M. A.; Tour, J. M. *Sci. Am.* **2000**, *282*, 86.
(12) Bumm, L. A.; Arnold, J. J.; Cygan, M. T.; Dunbar, T. D.; Burgin, T. P.; Jones, L., II; Allara, D. L.; Tour, J. M.; Weiss, P. S. *Science* **1996**, *271*, 1705.
(13) Reed, M. A.; Zhou, C.; Muller, C. J.; Burgin, T. P.; Tour, J. M. *Science* **1997**, *278*, 252.
(14) Cygan, M. T.; Dunbar, T. D.; Arnold, J. J.; Bumm, L. A.; Shedlock, N. F.; Burgin, T. P.; Jones, L., II; Allara, D. L.; Tour, J. M.; Weiss, P. S. *J. Am. Chem. Soc.* **1998**, *120*, 2721.
(15) Creager, S.; Yu, C. J.; Bamdad, C.; O'Connor, S.; MacLean, T.; Lam, E.; Chong, Y.; Olsen, G. T.; Luo, J.; Gozin, M.; Kayyem, J. F. *J. Am. Chem. Soc.* **1999**, *121*, 1059.
(16) Fan, F. F.; Yang, J.; Dirk, S. M.; Price, D. W.; Kosynkin, D.; Tour, J. M.; Bard, A. J. *J. Am. Chem. Soc.* **2001**, *123*, 2454.
(17) Huang, S.; Tour, J. M. *J. Org. Chem.* **1999**, *64*, 8898.
(18) Jones, L., II; Schumm, J. S.; Tour, J. M. *J. Org. Chem.* **1997**, *62*, 1388.
(19) Ziener, U.; Godt, A. *J. Org. Chem.* **1997**, *62*, 6137.
(20) Kukula, H.; Veit, S.; Godt, A. *Eur. J. Org. Chem.* **1999**, 277.
(21) Bunz, U. H. F. *Chem. Rev.* **2000**, *100*, 1605.
(22) Huang, S.; Tour, J. M. *Tetrahedron Lett.* **1999**, *40*, 3347.
(23) Tour, J. M. *Chem. Rev.* **1996**, *96*, 537.
(24) Weder, C.; Wrighton, M. S. *Macromolecules* **1996**, *29*, 5157.
(25) Francke, V.; Mangel, T.; Müllen, K. *Macromolecules* **1998**, *31*, 2447.
(26) Kloppenburg, L.; Jones, D.; Claridge, J. B.; Loye, H.-C.; Bunz, U. H. F. *Macromolecules* **1999**, *32*, 4460.
(27) Liu, C. Y.; Bard, A. *Acc. Chem. Res.* **1999**, *32*, 235.
(28) Lovinger, A. J.; Lotz, B.; Davis, D. D.; Schumacher, M. *Macromolecules* **1994**, *27*, 6603.
(29) Tsukruk, V. V.; Reneker, D. H. *Macromolecules* **1995**, *28*, 1370.
(30) Liu, T. X.; Zhou, C. Z.; Tjiu, W. C.; Chen, Z. K. Unpublished results.
(31) Moroni, M.; LeMoigne, J.; Luzzati, S. *Macromolecules* **1994**, *27*, 562.

(32) Meier, H.; Ickenroth, D.; Stalmach, U.; Koynov, K.; Bahtiar, A.; Bubeck, C. *Eur. J. Org. Chem.* **2001**, *23*, 4431.
(33) Ickenroth, D.; Weissmann, S.; Rumpf, N.; Meier, H. *Eur. J. Org. Chem.* **2002**, *16*, 2808.
(34) Li, H.; Powell, D. R.; Hayashi, R. K.; West, R. *Macromolecules* **1998**, *31*, 52.
(35) Sluch, M. I.; Godt, A.; Bunz, U. H. F.; Berg, M. A. *J. Am. Chem. Soc.* **2001**, *123*, 6447.
(36) Bao, Z.; Lovinger, A. J. *Chem. Mater.* **1999**, *11*, 2607.
(37) Hosaka, N.; Tachibaba, H.; Shiga, N.; Matsumoto, M.; Tokura, Y. *Phys. Rev. Lett.* **1999**, *82*, 1672.
(38) Sakurai, K.; Tachibana, H.; Shiga, N.; Terakura, C.; Matsumoto, M.; Tokura, Y. *Phys. Rev. B* **1997**, *56*, 9552.
(39) Trznadel, M.; Pron, A.; Zagorska, M.; Chrzaszcz, R.; Pielichowski, J. *Macromolecules* **1998**, *31*, 5051.
(40) Hernandez, V.; Castiglioni, C.; Del Zoppo, M.; Zerbi, G. *Phys. Rev. B* **1994**, *50*, 9815.
(41) Bredas, J. L.; Cornil, J.; Heeger, A. J. *Adv. Mater.* **1996**, *8*, 447.
(42) Meng, H.; Chen, Z.-K.; Huang, W. *J. Phys. Chem. B* **1999**, *103*, 6429.
(43) Halkyard, C. E.; Rampey, M. E.; Kloppenburg, L.; Studer-Martinez, S. L.; Bunz, U. H. F. *Macromolecules* **1998**, *31*, 8655.

MA021656A